DYNAMICAL MODELS AND NUMERICAL SIMULATIONS OF INCOMPLETE VIOLENT RELAXATION

M. TRENTI[1] & G. BERTIN[2]
(1) Scuola Normale Superiore, piazza dei Cavalieri 7, I-56126 Pisa, Italy;
(2) Dipartimento di Fisica, Università di Milano, via Celoria 16, I-20133 Milano, Italy

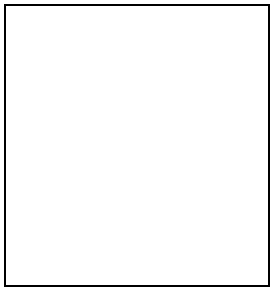

N-body simulations of collisionless collapse have offered important clues to the construction of realistic stellar dynamical models of elliptical galaxies. Such simulations confirm and quantify the qualitative expectation that rapid collapse of a self-gravitating collisionless system, initially cool and significantly far from equilibrium, leads to incomplete relaxation. In this paper we revisit the problem, by comparing the detailed properties of a family of distribution functions derived from statistical mechanics arguments to those of the products of collisionless collapse found in N-body simulations.

1 Introduction

The collapse of a dynamically cold cloud of stars can lead to the formation of realistic stellar systems, with projected density profiles well represented by the $R^{1/4}$ law [13]. The theoretical framework for the mechanism of incomplete violent relaxation that governs this scenario of structure formation was proposed by Lynden-Bell [9], who argued that fast fluctuations of the potential during collapse would lead to the formation of a well-relaxed isotropic core, embedded in a radially anisotropic, partially relaxed halo. This general picture served as a physical justification for the construction of the so-called f_∞ models [3], which indeed recovered the $R^{1/4}$ law and, suitably extended to the case of two-component systems (to account for the coexistence of luminous and dark matter), led to a number of interesting applications to the observations [4].

The application of statistical mechanics to this formation scenario [10] also led to the derivation of a separate family of distribution functions, the $f^{(\nu)}$ models, which was recently shown to possess interesting thermodynamic properties in the context of the gravothermal catastrophe [5]. The key ingredient for the construction of the $f^{(\nu)}$ models is the conjecture that a *third* quantity Q (defined as $Q = \int J^\nu |E|^{-3\nu/4} f d^3q d^3p$), in addition to the total mass M and the

total energy E_{tot}, is *approximately* conserved during the process of collisionless collapse. This quantity is introduced to model the process of *incomplete* violent relaxation, ensuring a radially biased pressure tensor and a $1/r^4$ density profile in the outer parts of the system. A preliminary inspection of the general characteristics of the $f^{(\nu)}$ models then convinced us that, with significant advantage over the f_∞ models, they might also serve as a good framework to interpret the results of simulations of collisionless collapse not only qualitatively, but also in quantitative detail, which is the main point of this paper.

2 Models

The extremization of the Boltzmann entropy under the three constraints described in the previous section leads to the distribution function $f^{(\nu)} = A \exp\left[-aE - d(J^2/|E|^{3/2})^{\nu/2}\right]$, where a, A, d, and ν are positive real constants; here E ($E < 0$) and J denote single-star specific energy and angular momentum. At fixed value of ν, one may think of these constants as providing two dimensional scales (for example, M and Q) and one dimensionless parameter, such as $\gamma = ad^{2/\nu}/(4\pi GA)$. In the following we will focus on values of ν ranging from 3/8 to 1. The corresponding models are constructed by solving the Poisson equation for the self-consistent mean potential $\Phi(r)$ generated by the density distribution associated with $f^{(\nu)}$. At fixed value of ν, the models thus generated make a one-parameter family of equilibria, described by the concentration parameter $\Psi = -a\Phi(0)$, the dimensionless depth of the central potential well. The projected density profile of concentrated models is well fitted by the $R^{1/n}$ law, with n close to 4, and the models provide reasonable fits to the surface brightness and to the kinematic profiles of bright elliptical galaxies [12].

3 Simulations of collisionless collapse

In principle, to study the process of collisionless collapse we have two options: either a tree code [1] or a particle-mesh [13] algorithm. We are interested in the large scale structure of the end-products of collisionless collapse, for systems that do not exhibit large deviations from spherical symmetry. The natural choice thus appears to be that of a particle-mesh code, based on a spherical grid and an expansion in spherical harmonics. The code used in the present study is thus a new version [11] of the van Albada code. For completeness, we have also run a number of comparison simulations with the fast code developed by Dehnen [7], which confirmed that our results do not depend on the numerical scheme employed.

During the process of collisionless collapse, violent relaxation is expected to wipe out much of the details that characterize the initial conditions, so that the end-products are expected to have properties that depend only or mostly on the initial value of the virial ratio $u = (2K/|W|)_{t=0}$, which sets the relevant collapse factor. In reality, violent relaxation is incomplete. Therefore, the final state is that of an approximate dynamical equilibrium characterized by an anisotropic distribution function, different from a Maxwellian (which would correspond to thermodynamic equilibrium). Because of such incomplete relaxation, the end-products of the simulations do conserve some memory of the initial state.

Earlier investigations [13,8] compared "clumpy" to "homogeneous" initial conditions, showing that clumpy initial conditions lead to end-states with projected density distributions well fitted by the $R^{1/4}$ law. We argue that, if the degree of symmetry in the initial conditions is excessive, little room is left for the mechanism of violent relaxation; this is confirmed by the fact that little or no mixing is observed in the single-particle angular momentum for homogeneous simulations, as reported in Fig. 1. We have thus chosen to focus this paper on clumpy initial conditions, for which an efficient mixing in phase space is guaranteed.

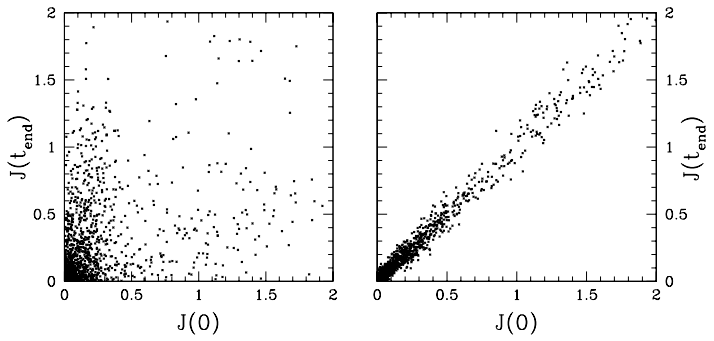

Figure 1: Single-particle angular momentum scatter (correlation between the initial and final values of J) for a typical clumpy simulation (left panel) and for its symmetrized (homogeneous) version (right panel). The symmetrization process in the initial state is performed by accepting the radius and the magnitude of the velocity of each particle, following the procedure for initial clumpy conditions, but by redistributing uniformly the angular variables.

We performed several runs varying the number of clumps and the initial virial ratio u in the range from 0.05 to 0.25. In most cases the clumps are cold, i.e. their kinetic energy is all associated with the motion of their centers of mass. The simulations are run for several dynamical times beyond the violent collapse phase, ensuring that the system has settled into a quasi-equilibrium. The final configurations are quasi-spherical, with shapes that resemble those of $E2-E3$ galaxies. The final equilibrium half-mass radius r_M is basically independent of the value of u. The central concentration achieved correlates with u, as can be inferred from the conservation of maximum density in phase space [8].

4 Fits and phase-space properties

In order to study the output of the simulations we compare the density and the anisotropy profiles, $\rho(r)$ and $\alpha(r)$ (here the local anisotropy is defined as $\alpha(r) = 2 - (\langle p_\theta^2 \rangle + \langle p_\phi^2 \rangle)/\langle p_r^2 \rangle$), of the end-products with the theoretical profiles of the $f^{(\nu)}$ family of models. Smooth simulation profiles are obtained by averaging over time in the last few dynamical times of the simulation. For the fitting models, the parameter space explored is that of an equally spaced grid in (ν, Ψ), with a subdivision of 1/8 in ν, from 3/8 to 1, and of 0.2 in Ψ, from 0.2 to 14.0; the mass and the half-mass radius of the models are fixed by the scales set by the simulations. A minimum χ^2 analysis is performed as described elsewhere [6].

As illustrated in Fig. 2, the density of the simulations is well represented by the best-fit $f^{(\nu)}$ profile over the entire radial range. The fit is satisfactory not only in the outer parts, where the density falls by *nine orders of magnitude* with respect to the center, but also in the inner regions. Depending on the initial virial parameter u, the end-products possess a density profile which, projected along the line-of-sight, may exhibit an $R^{1/n}$ behavior with different values of n and yet it is well fitted by the $f^{(\nu)}$ models. In turn, this may be interpreted in the framework of the proposed weak homology of elliptical galaxies [2].

To some extent, the final anisotropy profiles for clumpy initial conditions are found to be sensitive to the detailed choice of initialization, in particular to the number and the size of the clumps. The agreement between end-products of the collapse and models (see Fig. 2) seems to be best for simulations with 10 to 20 clumps, for a clump size such that the sum of their volumes fills the sphere where their centers of mass lie. We should recall that both the low and the high number of clumps limits are those of an initial homogeneous condition, unfavorable to violent relaxation.

At the level of phase space, we have performed two types of comparison, one involving the

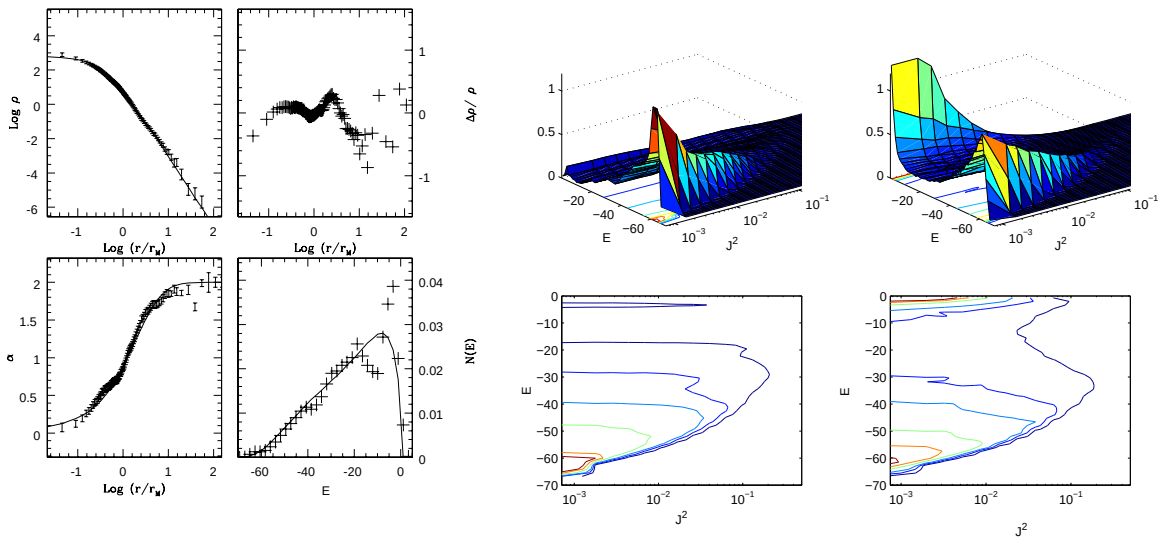

Figure 2: Comparison between the results of one simulation with $u = 0.23$, called $C2\_4$ (starting from 20 cold clumps), and the best-fit $f^{(\nu)}$ model ($\nu = 5/8$, $\Psi = 5.4$). *Left set of four panels.* Density as measured from the simulation (error bars) and model profile (top left). Residuals from the best-fit profile (top right). Anisotropy profile of the simulation (error bars) and profile (bottom left). Energy density distribution $N(E)$ (bottom right). *Right set of four panels.* Final phase space density $N(E, J^2)$ (left column), compared with that of the best fitting $f^{(\nu)}$ model (right column). The model curve for $N(E)$ and surface for $N(E, J^2)$ have been computed by a Monte Carlo sampling of phase space.

energy density distribution $N(E)$ and the other based on $N(E, J^2)$. The chosen normalization factors are such that: $M = \int N(E)dE = \int N(E, J^2)dEdJ^2$. In Fig. 2 we plot the final energy density distribution for a simulation run called $C2\_4$ with respect to the predictions of the best-fit model identified from the study of the density and pressure anisotropy distributions. The agreement is good, especially for strongly bound particles. At the deeper level of $N(E, J^2)$, simulations and models also agree quite well, as illustrated in the right set of four panels of Fig. 2. For the case shown, the distribution contour lines basically match in the range from E_{min} to $E \approx -30$ (in the relevant units); however, the theoretical model shows a peak located near the origin, not observed in the simulations.

References

1. Barnes, J., Hut, P., Nature **324**, 466 (1986)
2. Bertin, G., Ciotti, L., Del Principe, M., Astron. Astrophys. **386**, 149 (2002)
3. Bertin, G., Stiavelli, M., Astron. Astrophys. **137**, 26 (1984)
4. Bertin, G., Stiavelli, M., Rep. Prog. Phys. **56**, 493 (1993)
5. Bertin, G., Trenti, M., Astrophys. J. **584**, 729 (2003)
6. Bertin, G., Trenti, M., AIP Conf. Proc. **703**, 318 (2004)
7. Dehnen, W., Astrophys. J. Letters **536**, L39 (2000)
8. Londrillo, P., Messina, A., Stiavelli, M., Mon. Not. Roy. Astron. Soc. **250**, 54 (1991)
9. Lynden-Bell, D., Mon. Not. Roy. Astron. Soc. **136**, 101 (1967)
10. Stiavelli, M., Bertin, G., Mon. Not. Roy. Astron. Soc. **229**, 61 (1987)
11. Trenti, M., Ph.D. Thesis, Scuola Normale Superiore, Pisa, in preparation
12. Trenti, M., Bertin, G., submitted (2004)
13. van Albada, T.S., Mon. Not. Roy. Astron. Soc. **201**, 939 (1982)